Science Advances
AAAS

advances.sciencemag.org/cgi/content/full/6/22/eaaz3865/DC1

Supplementary Materials for

RNA binding protein PCBP1 is an intracellular immune checkpoint for shaping T cell responses in cancer immunity

Ephraim A. Ansa-Addo*, Huai-Cheng Huang, Brian Riesenberg, Supinya Iamsawat, Davis Borucki, Michelle H. Nelson, Jin Hyun Nam, Dongjun Chung, Chrystal M. Paulos, Bei Liu, Xue-Zhong Yu, Caroline Philpott, Philip H. Howe, Zihai Li*

*Corresponding author. Email: ephraim.ansa-addo@osumc.edu (E.A.A.-A); zihai.li@osumc.edu (Z.L.)

Published 29 May 2020, *Sci. Adv.* **6**, eaaz3865 (2020)
DOI: 10.1126/sciadv.aaz3865

This PDF file includes:

Figs. S1 to S8
Table S1

Ansa-Addo and Huang *et al*

Suppl Figure 1

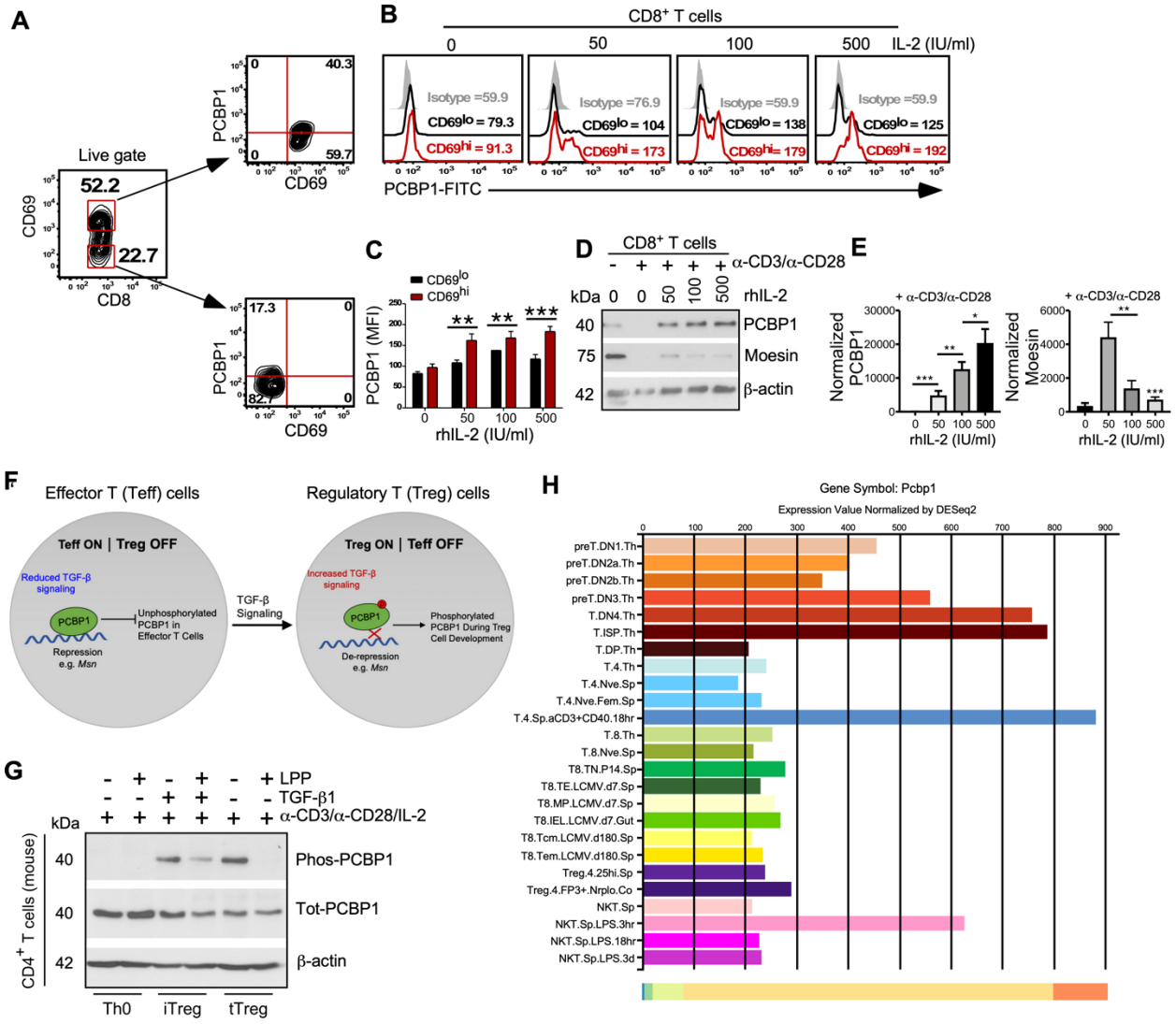

Fig. S1. Activation-induced and TGF-β-mediated phosphorylation of PCBP1 in T cells. (**A-E**) Splenic isolated CD8^{+} T cells cultured *in vitro* for 3 days with polyclonal anti-CD3/anti-CD28 antibodies and increasing concentrations of IL-2. Representation flow cytometry of PCBP1 expression in CD69^{low} and CD69^{high} T cells (A and B), and quantification (C). Immunoblotting (D) and quantification (E) for moesin, PCBP1 and β-actin after 3 days. (**F**) Model depicting unphosphorylated PCBP1 in effector T cells (left) under reduced TGF-β conditions, and

phosphorylated PCBP1 under settings of increased TGF-β signaling (right). (**G**) Immunoblotting for phosphorylated (Phos-PCBP1) and total PCBP1 (Tot-PCBP1) in $CD4^+$ T cells polarized *in vitro* without TGF-β (Th0) or with TGF-β (iTreg) for 3 days, as well as splenic Treg cells (tTregs) before and after incubation with lambda protein phosphatase (LPP). β-actin is used as a loading control. (**H**) Expression of *PCBP1* mRNA in the thymus and peripheral lymphoid organs normalized by DESeq2 - obtained from the Immunological Genome Project (www.immgen.org). (C and E) Error bars represent the mean ± SD; **P* < 0.05, ***P* < 0.01, ****P* < 0.001 (Student's t test); ns, not significant.

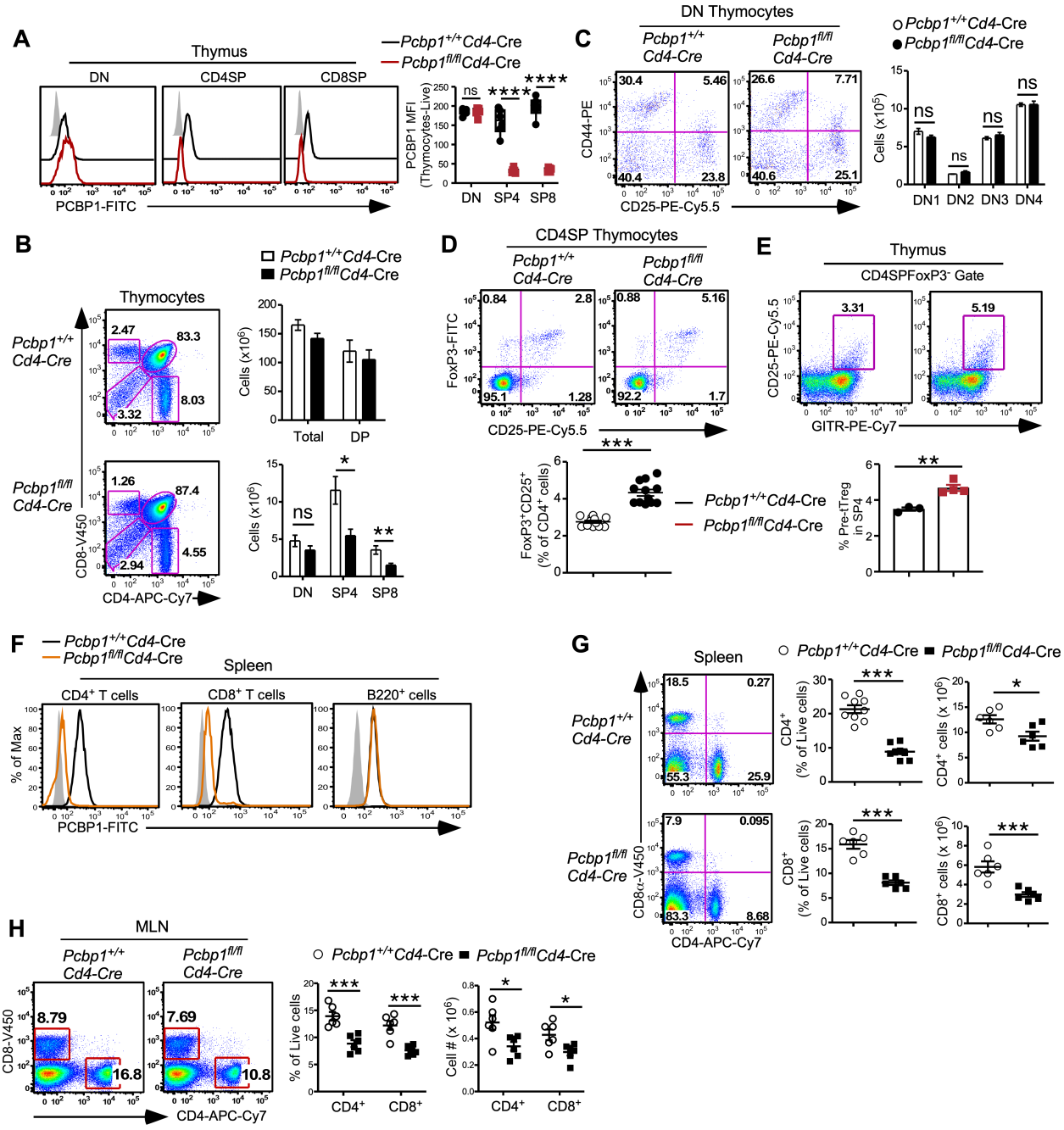

Fig. S2. Involvement of PCBP1 in T cell development and proliferation. (**A**) Flow cytometry for PCBP1 expression in DN, SP4, SP8 thymocytes and quantification; n=6. (**B**) Analysis of CD4 and CD8 on thymocytes (left) and quantification (right) of cells in various subsets of thymocytes derived from *Pcbp1*$^{+/+}$*Cd4*-Cre and *Pcbp1*$^{fl/fl}$*Cd4*-Cre mice (n= 6). (**C**) Flow cytometry analysis of

CD44 and CD25 on DN thymocytes (left) and quantification of various subsets (right), n= 6. No significance versus wild-type, Student's t test. (**D**) Intracellular FoxP3 and cell-surface CD25 (top) and the percentage of $FoxP3^{+}CD25^{+}$ cells (bottom) among $CD4^{+}CD8^{-}$ thymocytes from *Pcbp1*$^{+/+}$C*d4*-Cre and *Pcbp1*$^{fl/fl}$C*d4*-Cre mice (n= 12). (**E**) Analysis of CD25 and GITR pre-Treg cells on CD4SPFoxP3^{-} thymocytes and quantification. (**F**) Expression of PCBP1 in $CD4^{+}$, $CD8^{+}$, $B220^{+}$ splenic cells comparing *Pcbp1*$^{f/f}$ and *Pcbp1*$^{f/f}$*Cd4*-Cre mice, n= 6. (**G**) Flow cytometry analysis of CD4 and CD8 (left) on the proportion (middle) and number (right) of splenocytes in *Pcbp1*$^{+/+}$C*d4*-Cre and *Pcbp1*$^{fl/fl}$C*d4*-Cre mice (n= 8). (**H**) Flow cytometry analyzing the proportion of CD4 and CD8 (left) and number (right) on live lymph node cells; n= 6. Error bars represent the mean ± SE (A-E, G and H); **P* < 0.05, ***P* < 0.01; ****P* < 0.001 (Student's t test); ns, not significant.

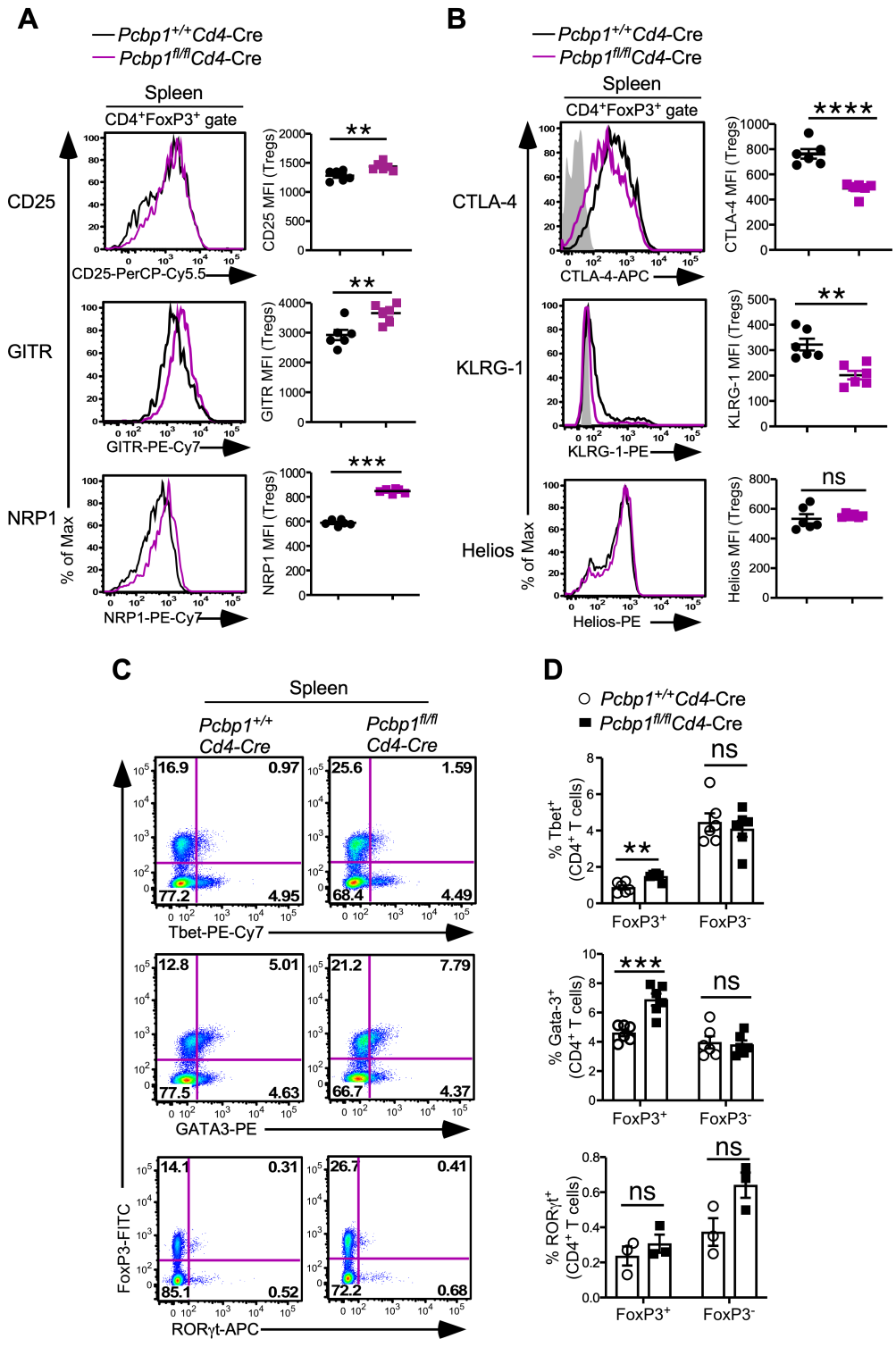

Fig. S3. Expression of Treg signature molecules and T cell subsets. (**A**) Flow cytometry analyzing the expression of CD25, GITR and NRP1 (left) and quantified (right) on splenic CD4^{+}FoxP3^{+} Tregs from *Pcbp1*$^{f/f}$ and *Pcbp1*$^{f/f}$*Cd4*-Cre mice, n= 6. (**B**) Expression of intracellular

CTLA-4, Helios and surface KLRG-1 GITR and NRP1 (left) and quantified (right) on splenic $CD4^+FoxP3^+$ Tregs from *Pcbp1*$^{f/f}$ and *Pcbp1*$^{f/f}$*Cd4*-Cre mice, n= 6. (**C** and **D**) Flow cytometry analyzing $Tbet^+$, GATA-3^+ and $ROR\gamma t^+$ cells (C) and the percentages (D) among splenic $CD4^+FoxP3^+$ and $CD4^+FoxP3^-$ T cells. Error bars represent the mean ± SE (A, B and D); $^{**}P < 0.01$; $^{***}P < 0.001$, $^{****}P < 0.0001$ (Student's t test); ns, not significant.

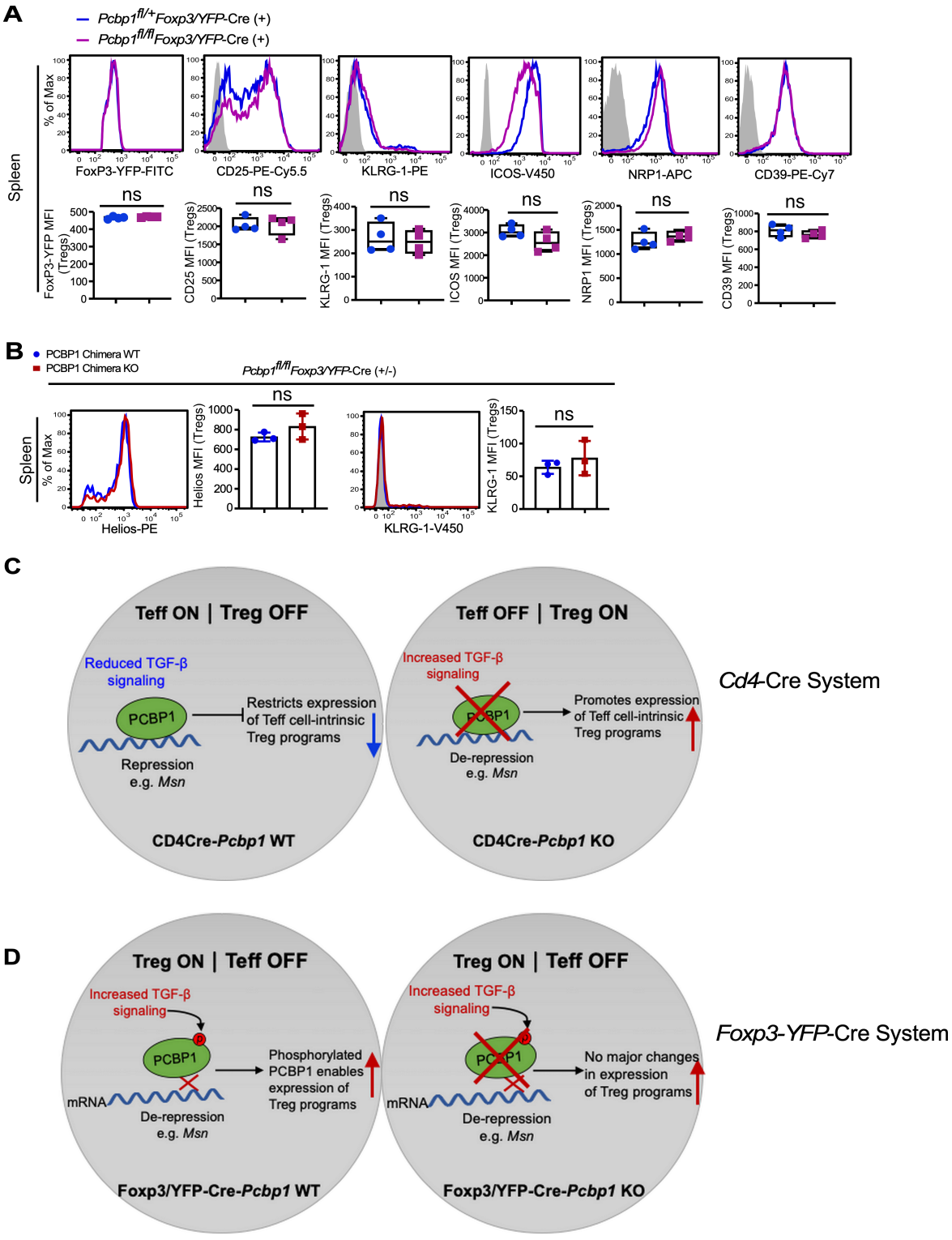
A
Pcbp1fl/+Foxp3/YFP-Cre (+)
Pcbp1fl/flFoxp3/YFP-Cre (+)
Spleen
% of Max
FoxP3-YFP-FITC
CD25-PE-Cy5.5
KLRG-1-PE
ICOS-V450
NRP1-APC
CD39-PE-Cy7
FoxP3-YFP MFI (Tregs)
CD25 MFI (Tregs)
KLRG-1 MFI (Tregs)
ICOS MFI (Tregs)
NRP1 MFI (Tregs)
CD39 MFI (Tregs)
ns
B
PCBP1 Chimera WT
PCBP1 Chimera KO
Pcbp1fl/flFoxp3/YFP-Cre (+/-)
Helios-PE
Helios MFI (Tregs)
KLRG-1-V450
KLRG-1 MFI (Tregs)
C
Teff ON | Treg OFF
Reduced TGF-β signaling
PCBP1
Restricts expression of Teff cell-intrinsic Treg programs
Repression
e.g. Msn
CD4Cre-Pcbp1 WT
Teff OFF | Treg ON
Increased TGF-β signaling
Promotes expression of Teff cell-intrinsic Treg programs
De-repression
e.g. Msn
CD4Cre-Pcbp1 KO
Cd4-Cre System
D
Treg ON | Teff OFF
Increased TGF-β signaling
P
Phosphorylated PCBP1 enables expression of Treg programs
mRNA
De-repression
e.g. Msn
Foxp3/YFP-Cre-Pcbp1 WT
No major changes in expression of Treg programs
Foxp3/YFP-Cre-Pcbp1 KO
Foxp3-YFP-Cre System

Fig. S4. PCBP1 in Tregs is redundant for Treg cell maintenance. (**A**) Flow cytometry analyzing the expression of Treg signature molecules CD25, KLRG-1, ICOS, NRP1 and CD39 (top) and quantification (bottom) in FoxP3/YFP^{+} Treg cells from the spleen of *Pcbp1*$^{f/+}$*Foxp3/YFP*-Cre^{+} and *Pcbp1*$^{f/f}$*Foxp3/YFP*-Cre^{+} littermate mice, n= 4. (**B**) Detection of surface KLRG-1 and intracellular Helios expression (left) with quantification (right) *in Pcbp1*$^{f/f}$*Foxp3/YFP*-Cre$^{+/-}$ chimera mice gating on PCBP1 chimera WT and PCBP1 chimera KO from the spleen, n= 3. (**C** and **D**) Models depicting effects of PCBP1 deletion using the *Cd4*-Cre (C) and *Foxp3-YFP*-Cre (D) genetic systems. Error bars represent the mean ± SE (A and B); ns, not significant (Student's t test).

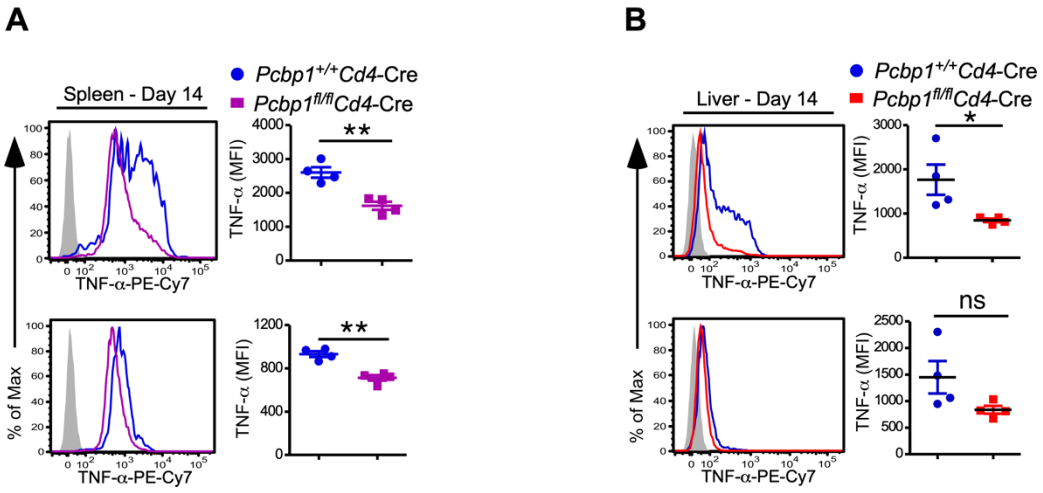

Fig. S5. Loss of PCBP1 promotes conversion of activated T cells into Tregs and impairs effector T cell functions. (**A** and **B**) Flow cytometry assessment of TNF-α expression (left) and quantified (right) of $CD4^+$ and $CD8^+$ T cells from the spleen (A) and liver (B) of *Pcbp1*$^{f/f}$ and *Pcbp1*$^{f/f}$*Cd4*-Cre littermate mice, n= 4. Error bars represent mean ± SEM (A and B); $*P < 0.05$, $**P < 0.01$ (Student's t test); ns, not significant.

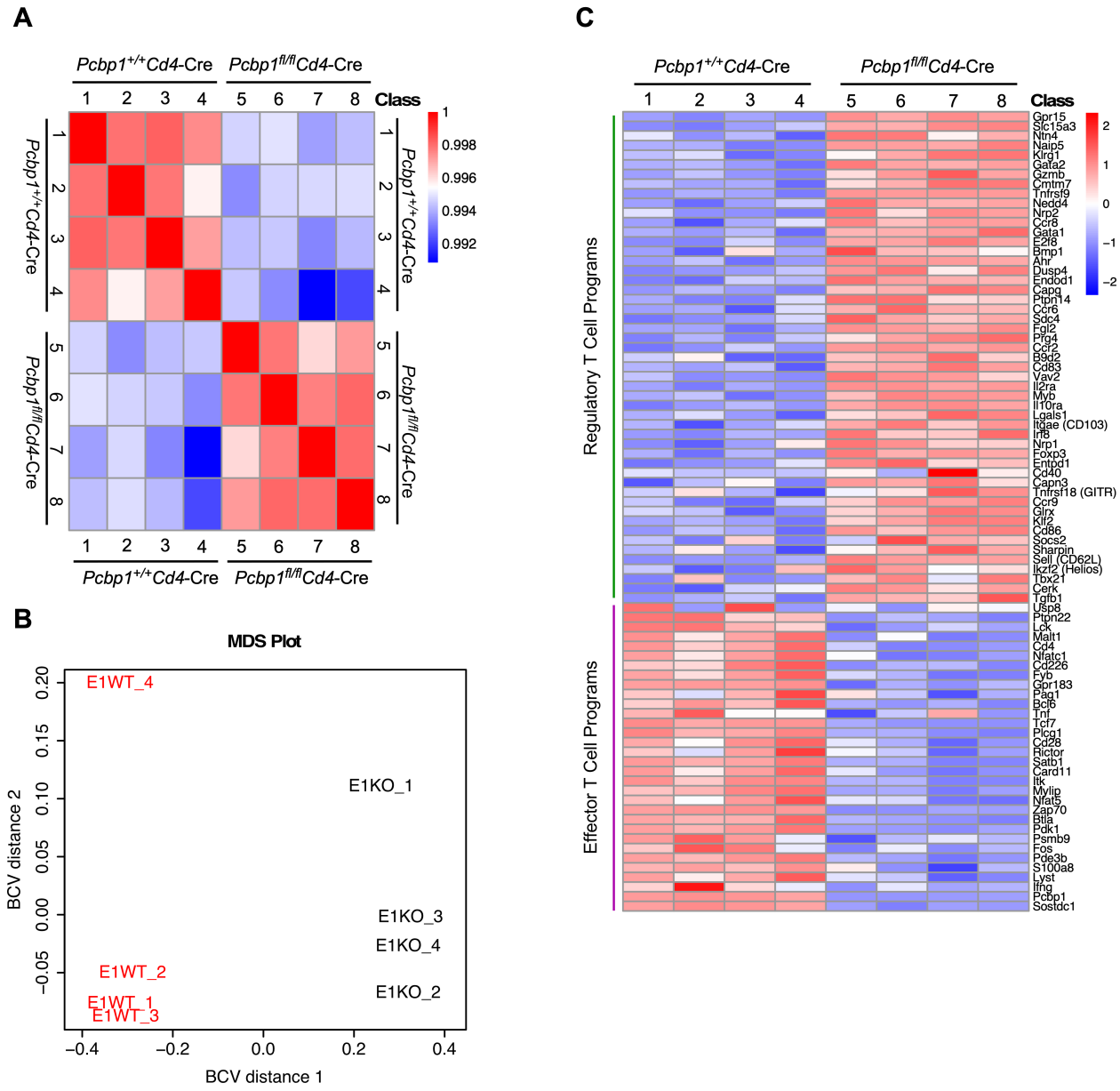

Fig. S6. RNA-seq data analysis and quality control. (**A**) Correlation plot of a log10-transformed counts per million (CPM) of eight RNA-seq samples from CD4$^+$ T cells isolated from the spleen of *Pcbp1*$^{f/f}$ and *Pcbp1*$^{f/f}$*Cd4*-Cre littermate mice showing high reproducibility at 99%. (**B**) MDS plot of a log2-transformed CPM of eight RNA-seq samples. (**C**) Heat map of Treg and Teff cell-signature genes in CD4$^+$ T cells isolated from the spleen of 6-8 weeks old *Pcbp1*$^{f/f}$ and *Pcbp1*$^{f/f}$*Cd4*-Cre littermate mice.

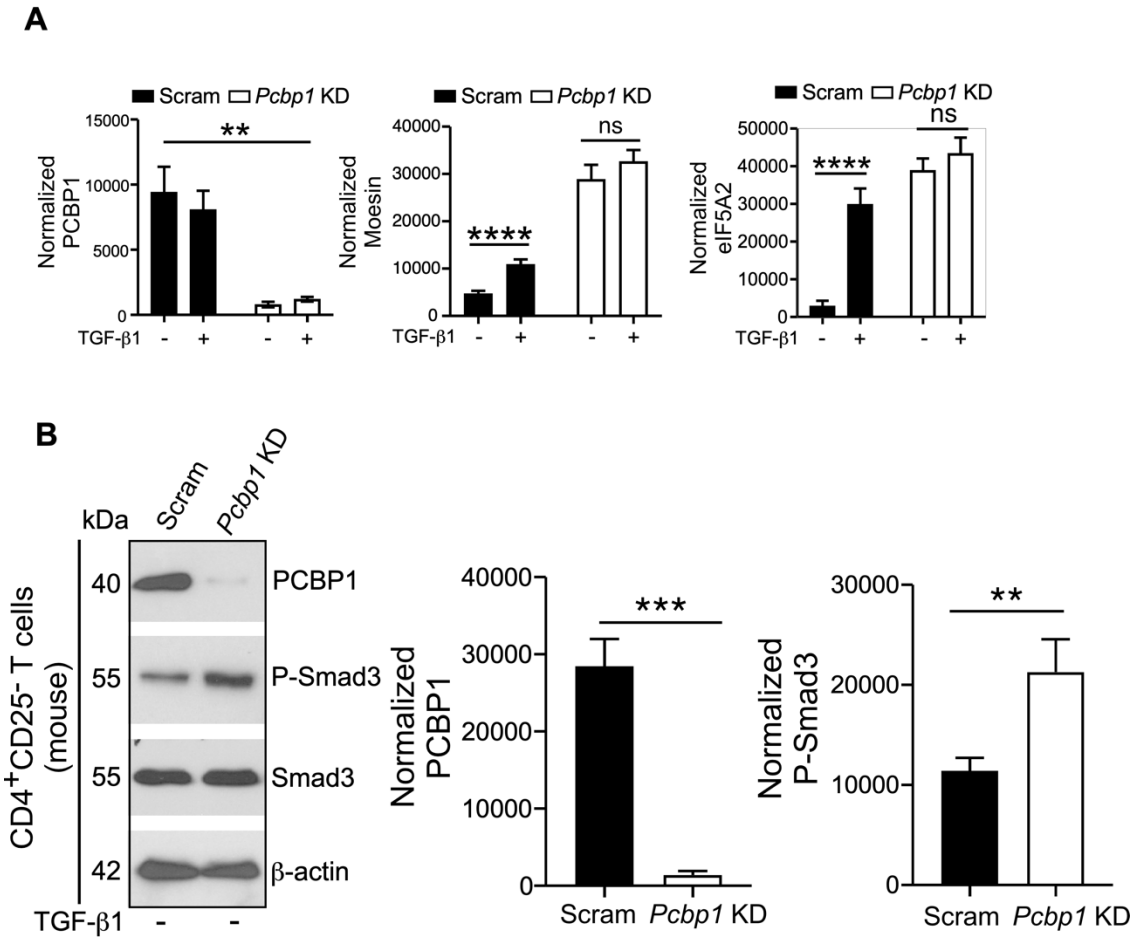

Fig. S7. Inhibition of PCBP1 promotes TGF-β signaling in T cells. (**A**) Quantified data of PCBP1, moesin and eIF5A2 for immunoblotting on Fig. 5 A. (**B**) Immunoblotting of PCBP1 and phosphorylated-Smad3 (P-Smad3), and total Smad3, and quantification using $CD4^{+}CD25^{-}$ T cells transduced with scrambled (scram) vector, or lentiviral shRNA targeting *Pcbp1* in the absence of TGF-β, but with anti-CD3/anti-CD28 antibody. Error bars represent the mean ± SE of independent experiments. $^{**}P < 0.01$; $^{***}P < 0.001$ (Student's t test); ns, no significance.

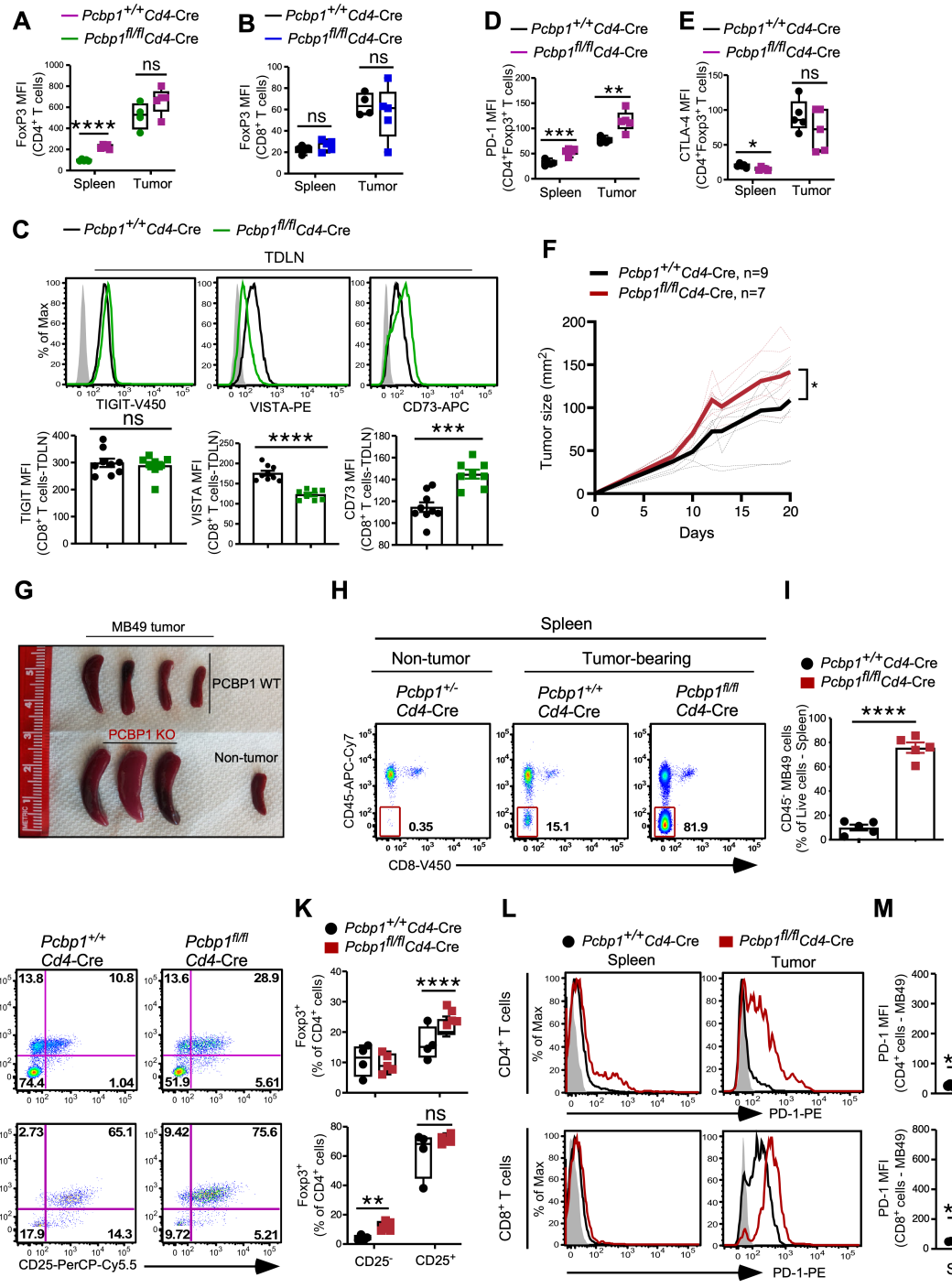

Fig. S8. Absence of PCBP1 in T cells promotes immune suppression and impairs anti-tumor T cell responses. (**A** and **B**) Flow cytometry analyzing FoxP3 expression in CD4$^+$ (A) and CD8$^+$ (B) T cells isolated from the spleen and tumor of *Pcbp1*$^{f/f}$ (n= 4) and *Pcbp1*$^{f/f}$*Cd4*-Cre (n= 5) mice. (**C**) Flow cytometric analysis (top) and quantification (bottom) of TIGIT, VISTA and CD73

expression in $CD8^+$ T cells from the TDLN. Control (n= 9) and *Pcbp1*$^{fl/fl}$C*d4*-Cre mice (n= 8). (**D** and **E**) Analyzed surface expression of the inhibitory checkpoint receptors, PD-1 (D) and CTLA-4 (E) in $CD4^+FoxP3^+$ T cells isolated from the spleen and tumor of *Pcbp1*$^{f/f}$ and *Pcbp1*$^{f/f}$*Cd4*-Cre mice, n= 5). (**F** and **G**) Tumor growth curve of wild-type control and *Pcbp1*$^{fl/fl}$C*d4*-Cre mice that received orthotopic injection of MB49 cells in a bladder cancer model (F) and spleen size at endpoint (G). Photo credit: E.A. Ansa-Addo (The Ohio State University). (**H** and **I**) Presence of $CD45^-$ cells (H) and quantification (I) in the spleen of non-tumor bearing and tumor-bearing wild-type (n= 9) and *Pcbp1*$^{fl/fl}$C*d4*-Cre mice (n= 7) at endpoint day 20 determined by flow cytometry. (**J** and **K**) Frequency of $FoxP3^+$ expressing T cells (J) and quantification (K) among $CD25^-$ and $CD25^+$ T cells isolated from the spleen and tumor of *Pcbp1*$^{f/f}$*Cd4*-Cre compared with tumor-bearing *Pcbp1*$^{f/f}$ littermate mice. (**L** and **M**) Flow cytometry of PD-1 expression (L) and quantification (M) on $CD4^+$ and $CD8^+$ T cells from spleens and tumors collected from control and *Pcbp1*$^{f/f}$*Cd4*-Cre mice, n= 6. Error bars represent the mean ± SE (A-E, I, K and M). **P* < 0.05; ***P* < 0.01; ****P* < 0.001; *****P* < 0.0001 (Student's t test); (F) Two-way analysis of variance (AVONA); ns, no significance.

Table S1. Key Reagents

REAGENT or RESOURCE	SOURCE	IDENTIFIER
Antibodies		
Anti-B220-FITC (clone RA3-6B2)	BioLegend	Cat#:103206; RRID:AB_312991
Anti-CD127-APC-Cy7 (clone A7R34)	BioLegend	Cat#:135039; RRID: AB_2566160
Anti-CD24-FITC (clone M1/69)	BD Biosciences	Cat#:553261; RRID: AB_394740
Anti-CD25-PE (clone PC61)	BioLegend	Cat#:102008; RRID: AB_312857
Anti-CD25-PE-Cy5.5 (clone PC61.5)	eBioscience	Cat#:35-0251-82; RRID: AB_11218898
Anti-CD28 functional (clone 37.51)	BioLegend	Cat#:102110; RRID: AB_312875
Anti-CD3 functional (clone 145-2C11)	BioLegend	Cat#:557306; RRID: AB_1877073
Anti-CD39-PE-Cy7 (clone 24DMs1)	eBioscience	Cat#:25-0391-82; RRID: AB_1210766
Anti-CD44-PE (clone IM7)	BioLegend	Cat#:103008; RRID: AB_312959
Anti-CD45-APC-Cy7 (clone 30-F11)	BD Biosciences	Cat#:557659; RRID: AB_396774
Anti-CD4-APC-Cy7 (clone GK1.5)	BD Biosciences	Cat#:552051; RRID: AB_394331
Anti-CD4-PerCP-Cy5.5 (clone RM4-5)	eBioscience	Cat#:45-0042-82; RRID: AB_1107001
Anti-CD5-PE (clone 53-7.3)	eBioscience	Cat#:12-0051-82; RRID: AB_465523
Anti-CD62L-PE-Cy7 (clone MEL-14)	eBioscience	Cat#:25-0621-82; RRID: AB_469633
Anti-CD69-PE-Cy7 (clone H1.2F3)	BD Biosciences	Cat#:552879; RRID: AB_394508
Anti-CD73-APC (clone TY/11.8)	BioLegend	Cat#:127210; RRID: AB_11218786
Anti-CD8α-FITC (clone 53-6.7)	BD Biosciences	Cat#:11-0081-85; RRID: AB_464916
Anti-CD8α-V450 (clone 53-6.7)	eBioscience	Cat#:48-0081-82; RRID: AB_1272198
Anti-CTLA4-APC (clone UC10-4B9)	eBioscience	Cat#:17-1522-82; RRID: AB_2016700
Anti-CTLA4-PE (clone UC10-4F10-11)	BD Biosciences	Cat#: 553720; RRID: AB_395005
Anti-eIF5A2 antibody (clone D8L8Q)	Cell Signaling Technology	Cat#:20765; RRID: AB_2798849
Anti-Foxp3-APC (clone FJK-16s)	eBioscience	Cat#:17-5773-82; RRID: AB_469457
Anti-Foxp3-FITC (clone FJK-16s)	eBioscience	Cat#:11-5773-82; RRID: AB_465243

GARP Monoclonal Antibody (YGIC86), eFluor 450, eBioscience (TM)	Thermo Fisher	Cat# 48-9891-82, RRID: AB_10597007
Anti-GITR-PE (clone DTA-1)	eBioscience	Cat#:12-5874-82; RRID: AB_465986
Anti-GITR-PE-Cy7 (clone DTA-1)	eBioscience	Cat#:25-5874-82; RRID: AB_10548516
Anti-Helios-PE (clone 22F6)	eBioscience	Cat#:12-9883-42; RRID: AB_2572758
Anti-ICOS-V450 (clone 7E.17G9)	BD Biosciences	Cat#:564070; RRID: AB_2738576
Anti-IFN-γ functional (clone XMG1.2)	BioLegend	Cat#:505827; RRID: AB_2295769
Anti-IFNγ-PE (clone XMG1.2)	BD Biosciences	Cat#:555412; RRID: AB_395376
Anti-IFNγ-PerCP-Cy5.5 (clone 4S.B3)	BD Biosciences	Cat#:560742; RRID: AB_1727531
Anti-IL4 functional (clone 11B11)	BD Biosciences	Cat#:559062; RRID: AB_397187
Anti-Ki67-FITC	BD Biosciences	Cat#:612472; RRID: AB_399649
Anti-KLRG1-PE (clone 2F1)	eBioscience	Cat#:12-5893-82; RRID: AB_10596642
Anti-KLRG1-V450 (clone 2F1)	Invitrogen	Cat#:48-5893-82; RRID: AB_10852843
Anti-MHCI-APC (clone AF6-88.5.5.3)	eBioscience	Cat#:17-5958-82; RRID: AB_1311280
Anti-MHCII-FITC (clone M5/114.15.2)	eBioscience	Cat#:11-5321-85; RRID: AB_465233
Anti-Moesin antibody	Cell Signaling Technology	Cat#:3150; RRID: AB_2266802
Anti-mouse-IgG-FITC	eBioscience	Cat#:11-4011-85; RRID: AB_465218
Anti-mouse-IgG-PE (clone A85-1)	BD Biosciences	Cat#:550083; RRID: AB_393553
Anti-Nrp1-APC (clone 3DS304M)	eBioscience	Cat#:17-3041-82; RRID: AB_2573196
Anti-Nrp1-PE-Cy7 (clone 3DS304M)	eBioscience	Cat# 25-3041-82; RRID: AB_2573436
Anti-PCBP1 antibody	Cell Signaling Technology	Cat# 8534; RRID: AB_11129258
Anti-PD-1-APC (clone J43)	eBioscience	Cat# 17-9985-82; RRID: AB_11149358
Anti-PD-1-PE (clone J43)	BD Biosciences	Cat# 551892; RRID:AB_394284
Anti-pSmad2/3-APC (clone O72-670)	BD Biosciences	Cat# 562696; RRID: AB_2716578
Anti-Phospho-Smad3 Antibody (EP823Y)	Abcam	Cat# ab52903

Anti-Smad3 Antibody (EP568Y)	Abcam	Cat# ab40854
Anti-eIF5A2 (EPR7411-6)	Abcam	Cat# ab126735
Anti-RORγt-APC (clone B2D)	eBioscience	Cat# 17-6981-82; RRID: AB_2573254
REAGENT or RESOURCE	SOURCE	IDENTIFIER
Anti-Satb1-APC (clone 14/SATB1)	BD Biosciences	Cat# 562378; RRID: AB_11153310
Anti-T-bet-PE-Cy7 (clone 4B10)	eBioscience	Cat# 25-5825-8; RRID: AB_11042699
Anti-TCRβ-APC (clone H57-597)	BD Biosciences	Cat# 553174; RRID: AB_398534
Anti-TIGIT-V450 (clone 1G9)	BD Biosciences	Cat# 565270; RRID: AB_2688007
Anti-TNFα-PE-Cy7 (clone MP6-XT22)	BD Biosciences	Cat# 557644; RRID: AB_396761
Anti-VISTA-PE (clone MIH64)	BD Biosciences	Cat# 566269; RRID: AB_2744494
Chemicals, Peptides, and Recombinant Proteins		
Recombinant Human IL-2	PeproTech	Cat# 200-02
Recombinant Human IL-2	NIH Repository	N/A
Recombinant Human IL12p70	PeproTech	Cat# 200-12H
Recombinant Human TGF-β1	PeproTech	Cat# 100-21
PMA	Sigma Aldrich	Cat# P8139
Ionomycin	Sigma Aldrich	Cat# I0634
Fixable Viability Dye	eBioscience	Cat# 65-0866-14
Brefeldin A Solution (1000X)	ThermoFisher	Cat# 00-4506-51
ACK Lysing Buffer	Homemade	N/A
Critical Commercial Assays		
$CD4^+CD25^+$ Regulatory T Cell Isolation Kit, mouse	Miltenyi Biotec	Cat# 130-091-041
CD8a T Cell Isolation Kit, mouse	Miltenyi Biotec	Cat# 130-104-075
FoxP3/Transcription Factor Staining Buffer Set Kit	eBioscience	Cat# 00-5523-00
Dynabeads FlowComp Human CD4 Kit	Thermo Fisher	Cat# 11361D
Dynabeads FlowComp Human CD8 Kit	Thermo Fisher	Cat# 11362D
Dynabead Human T-Activator	Thermo Fisher	Cat# 11161D
eBioscience Fixable Viability Dye	Thermo Fisher	Cat# 65-0866-18
Genomic DNA clean & concentrator	QIAGEN	Cat# 28304
RNeasy Mini Kit	QIAGEN	Cat# 74104
Deposited Data		
RNA-Seq data	This paper	GEO: GSE131826
Experimental Models: Cells		

HEK293FT	ThermoFisher	Cat# R70007
Stbl3 competent cells	ThermoFisher	Cat# C737303

Experimental Models: Organisms/Strains

REAGENT or RESOURCE	SOURCE	IDENTIFIER
Mouse: Tg(Cd4-cre)1Cwi	Jackson Labs	JAX: 022071
Mouse: B6, *Pcbp1*$^{f/f}$*Foxp3*$^{YFP\text{-}Cre+}$	This paper	N/A
Mouse: B6, *Pcbp1*$^{f/f}$*Cd4*-Cre	This paper	N/A
Mouse: B6, *Pcbp1*$^{f/f}$*Foxp3*$^{YFP\text{-}Cre+/-}$	This paper	N/A
Mouse: C57BL6	Jackson Labs	Cat# 000664
Mouse: BALB/c	Charles River	Cat# 028
Mouse: NOD *Rag1*$^{-/-}$	Jackson Labs	Cat# 007799
Oligonucleotides		
shRNA targeting sequence: mouse *Pcbp1*: CCG GCC ATG ATC CAA CTG TGT AAT TCT CGA GAA TTA CAC AGT TGG ATC ATG GTT TTT G	This paper	N/A
Recombinant DNA		
pLKO.1 shRNA plasmid	Sigma-Aldrich	N/A
Software and Algorithms		
Flow Jo. v.8 & v.10	Tree Star Inc.	https://www.flowjo.com;RRID: SCR_008520
Prism v.5 & v.8	GraphPad	https://www.graphpad.com
edgeR software	Bioconductor	www.bioconductor.org/packages

CONTACT FOR REAGENT AND RESOURCE SHARING

Further information and requests for resources and reagents should be directed to and will be fulfilled by the Lead Contact, Dr. Zihai Li (Zihai.Li@osumc.edu).